Electronic supplementary information (ESI)

Theoretical Studies on the Strong Phonon Coherence in the Type-5 Penta-PbN_8 Sheet

Asghar Hussain, Chenxin Zhang, Peng-Hu Du, Qiang Sun*, Qian Wang*

S1. q-meshes used for convergent ShengBTE calculations of the penta-PbN_8 sheet

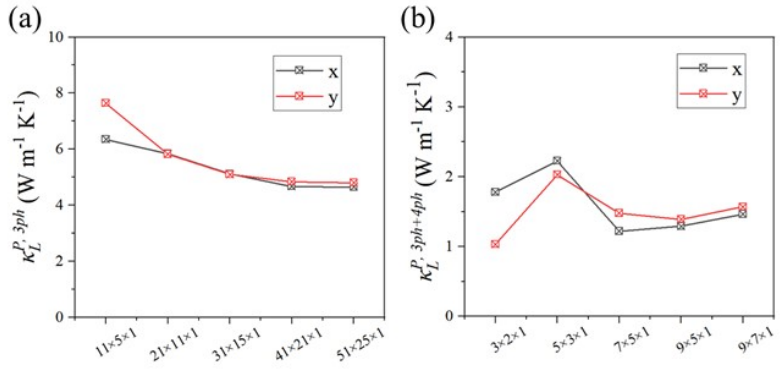

Fig. S1 Convergence test of the calculations for (a) 3- and (b) 3+4 phonon scattering processes of the penta-PbN_8 sheet.

S2. Convergence test for Hiphive fitting

We chose the cutoff distances of 8.17, 5.0 and 4.0 Å for second, third and fourth order IFCs, resulting in the best fitting RMSE of only 15.2 meV/Å, as shown Fig. S2. We also checked the effect of displacement amplitude by choosing the number of 0.01 and 0.02 Å for test. The calculated thermal conductivities within the same cutoff distances and *q*-mesh along *x*-direction are 1.29 and 1.12 W m^{-1} K^{-1} at 300 K, which are in good agreement with each other.

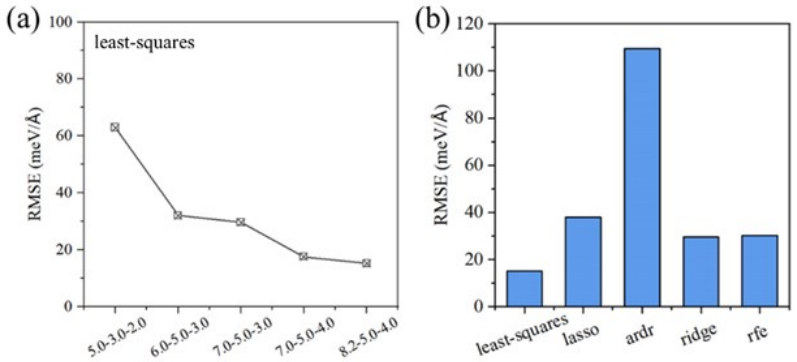

Fig. S2 (a) Convergence test of the cutoff distances for the fitted interatomic force constant potential, and (b) comparison of different fitting methods.[1]

S3. Theoretical model

In our calculations, we used projector-augmented wave (PAW) method augmented wave (PAW) pseudopotentials as implemented within the density functional theory (DFT) framework implemented in the Vienna *ab initio* simulation package (VASP) package, ensuring accurate representation of core-valence interactions for the elements in the material. To generate the force constant dataset for Hiphive, we used 100 structure samples created using a Monte Carlo displacement method, ensuring reliable representation of the configuration space for accurate anharmonic IFC fitting. The Brillouin zone was sampled using a Monkhorst-Pack *k*-point mesh of 3 × 3 × 1 with optimized k-point density to ensure total energy and forces convergence. The 2nd, 3rd, and 4th order IFC were fitted by conventional least-squares regression with cutoff distances set to 8.17 Å, 5.00 Å, and 4.00 Å, respectively.

S4. Convex-hull diagram of the Pb-N system

The formation energy of penta-PbN_8 (29 meV/atom) suggests it is energetically more favorable than PbN_6, which was already synthesized.[2]

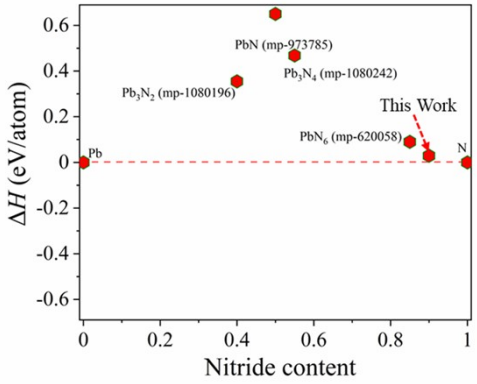

Fig. S3. The convex energy hull of the Pb_xN_{1-x} systems.

S5. Stiffness tensor matrix of the penta-PbN_8 sheet and its eigenvalues

Typically, the stiffness tensor components for a 2D material are used to form the stiffness tensor matrix as follows.

$$\mathbf{C} = \begin{pmatrix} C_{11} & C_{12} & C_{16} \\ C_{12} & C_{22} & C_{26} \\ C_{16} & C_{26} & C_{66} \end{pmatrix} \quad \text{(S1)}$$

For penta-PbN_8, the matrix reads

$$\mathbf{C}_{\text{penta-PbN}_8} = \begin{pmatrix} 74.48 & 70.05 & 0.29 \\ 70.05 & 34.91 & 0.24 \\ 0.29 & 0.24 & 0.27 \end{pmatrix} (\text{N}\cdot\text{m}^{-1}) . \quad \text{(S2)}$$

The eigenvalues of this matrix (λ_i, i = 1, 2, 3) and the corresponding normalized eigenvectors (x_i, i = 1, 2, 3) are as follows,

$$\begin{cases} \lambda_1 = 36.32\ \text{N}\cdot\text{m}^{-1} \\ \lambda_2 = 79.44\ \text{N}\cdot\text{m}^{-1} \\ \lambda_3 = 194.35\ \text{N}\cdot\text{m}^{-1} \end{cases}, \begin{cases} \boldsymbol{x}_1 = (-0.305, -0.005, 1)^{\dagger} \\ \boldsymbol{x}_2 = (3.381, -6.034, 1)^{\dagger} \\ \boldsymbol{x}_3 = (3.243, 1.983, 1)^{\dagger} \end{cases} . \quad \text{(S3)}$$

The positivity of all three eigenvalues indicates the mechanical stability of the penta-PbN_8 sheet as meeting the Born-Huang criteria. More precisely, any external strain can be expressed as a linear combination of x_1, x_2, and x_3 vectors, and the strain energy curve for each x_i vector follows a parabolic shape, with the quadratic term defined by $\lambda_i/2$. Consequently, the strain energy value remains consistently positive.

S6. Group velocity at different directions

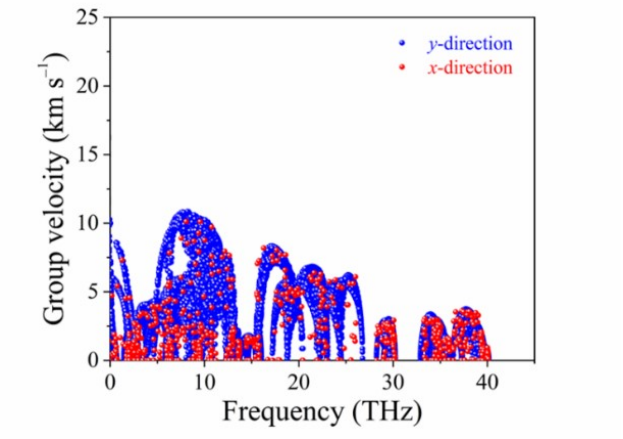

Fig. S4. Variations of the group velocities of the penta-PbN_8 sheet.

S7. Grüneisen parameter

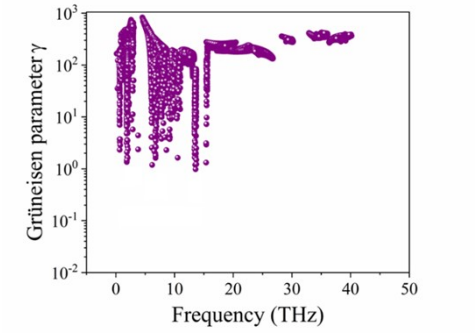

Fig. S5. Calculated Grüneisen parameter as a function of frequency for the penta-PbN_8 sheet.

S8. Three-phonon thermal conductivity

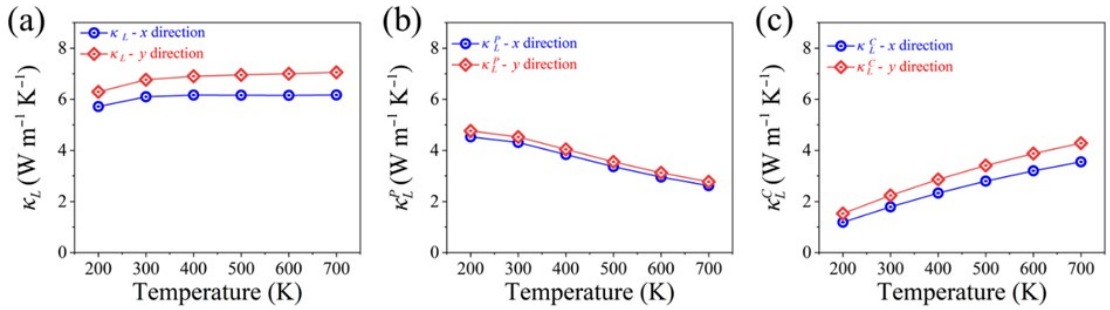

Fig. S6. (a) Total lattice thermal conductivity (κ_L), (b) particle-like contribution (κ_L^P), and (c) phonon coherence contribution (κ_L^C) considering three-phonon scattering of the penta-PbN_8 sheet.

S9. Mean free paths and lifetimes of the phonon modes

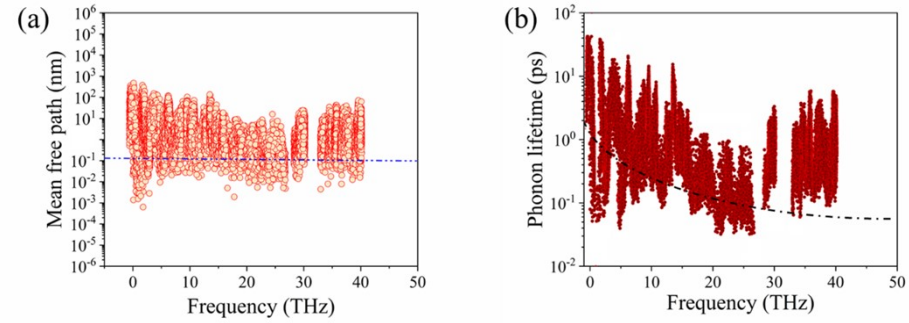

Fig. S7. Phonon means free path and phonon lifetime as a function of phonon frequency at 300 K for penta-PbN_8 sheet. The blue horizontal line is the average bond length (1.84 Å, Ioffe-Regel limits in space), and the black dashed curve is for the Ioffe-Regel limit ($1/\omega$) in time.

S10. Scattering rates with temperature

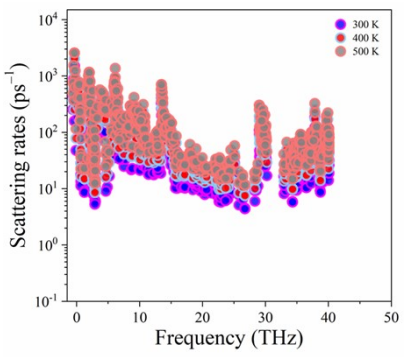

Fig. S8 Scattering rates of the penta-PbN_8 sheet at temperatures of 300, 400, and 500 K.

S11. Coherent lifetime (τ_{ij}) at 300 K and 500 K

The coherent lifetime is directly related to the wave-like nature of phonons and contributes to the coherent part of thermal conductivity, whereas the phonon lifetime captures the overall scattering processes. However, according to Eq. 5 (see manuscript), in certain regimes, stronger scattering can lead to larger coherent lifetimes. This occurs because increased scattering reduces the dominance of incoherent processes and allows some phonon modes to preserve coherence over longer timescales.

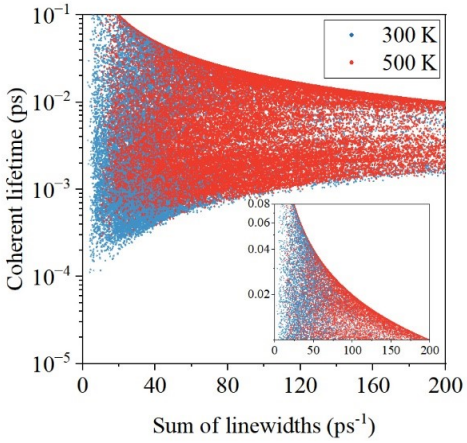

Fig. S9. Coherent lifetime (τ_{ij}) at 300 K and 500 K for the penta-PbN_8 sheet, the inset in the figure magnifies the high scattering rate region.

References

1. F. Eriksson, E. Fransson and P. Erhart, *Adv. Theory Simul.*, 2019, **2**, 1800184.
2. A. Jain, S. P. Ong, G. Hautier, W. Chen, W. D. Richards, S. Dacek, S. Cholia, D. Gunter, D. Skinner, and G. Ceder, Commentary: The Materials Project: A materials genome approach to accelerating materials innovation, *APL Mater.* 2013, **1**.